Large Angle Elastic Alpha Scattering on a $N = Z$ Nucleus above $A = 40$

K. E. Rehm, C. L. Jiang, I. Ahmad, J. Caggiano, P. Collon, J. P. Greene, D. Henderson, A. Heinz, R.V. F. Janssens, R. C. Pardo, T. Pennington, J. P. Schiffer, R. H. Siemssen, and A. H. Wuosmaa
Argonne National Laboratory, Argonne, Illinois 60439

M. Paul
Hebrew University, Jerusalem, Israel

P. Mohr
Technische Universität Darmstadt, D-64289 Darmstadt, Germany
(Received 6 May 2002; published 5 September 2002)

Scattering of alpha particles from ^{44}Ti, the lightest unstable alpha-particle nucleus above $A = 40$, has been measured at backward angles. The "anomalous" order-of-magnitude enhancement that is characteristic of ^{40}Ca and other light alpha-particle nuclei is not observed. Instead, the backward yield is similar to that observed for other nuclei heavier than ^{40}Ca, and is well described with average optical model parameters.

DOI: 10.1103/PhysRevLett.89.132501 PACS numbers: 25.60.Bx, 24.10.Ht, 25.55.Ci, 27.40.+z

Anomalous large angle scattering (ALAS) has been extensively studied in the past with α particles on *sd*-shell nuclei up to ^{40}Ca [1]. In ALAS, enhanced cross sections for elastic scattering are observed at angles beyond 90°. Different explanations of this effect have been proposed: α exchange [2], Regge poles [3], quasimolecular resonances [4], surface-transparent or L-dependent potentials [5], but also modified Woods-Saxon [6,7] or folding potentials [8]. From an analysis of all available data it appears that ALAS is a manifestation of weak absorption of the surface partial waves [9], but the origin of this surface transparency is not well understood. Because ALAS is especially pronounced for scattering of α particles on $N = Z$, α-particle nuclei (^{16}O, ^{20}Ne, ^{24}Mg, ^{28}Si, ^{32}S, ^{36}Ar, ^{40}Ca), it has been argued [2] that α cluster and exchange effects in the target nucleus might also play a role. Since no stable $N = Z$, α-particle nuclei exist beyond ^{40}Ca, the question whether ALAS ends at $A = 40$ could not be studied in the past. With the availability of suitable radioactive beams (e.g., the doubly magic $N = Z$ nucleus ^{56}Ni [10] or the nonmagic $N = Z$ nucleus ^{44}Ti [11]), the question about large backward angle cross sections for heavier $N = Z$ nuclei can now be addressed experimentally for the first time. While it was found that ^{41}Ca also showed enhanced backward scattering similar to ^{40}Ca [12], the enhancement disappears for ^{42}Ca and all other heavier nuclei. Slight changes in the character of the backward angle cross sections have been observed in α scattering on heavier closed-shell nuclei such as ^{90}Zr [13], or in heavy ion scattering on, e.g., ^{28}Si [14,15], but so far back angle elastic cross sections at or above the Rutherford values appear to be restricted to nuclei lighter than ^{40}Ca.

The smaller number of open channels in the (α, n) reaction which dominates the absorption [5] for ^{40}Ca ($Q_{\alpha,n} = -11.172$ MeV) has also been mentioned as an explanation for the reduced absorption when compared to ^{44}Ca with $Q_{\alpha,n} = -2.184$ MeV [1,5]. If a lack of open channels alone accounts for this phenomenon, elastic α scattering on heavier $N = Z$ nuclei, such as ^{44}Ti should also lead to enhanced cross sections at backward angles because the Q value is similarly negative ($Q_{\alpha,n} = -8.642$ MeV).

A beam of radioactive ^{44}Ti with intensities of $\sim 5 \times 10^5$ particles/s has recently been developed at the ATLAS accelerator at Argonne National Laboratory [11]. Although these beam intensities are small when compared to beams of stable particles, they nevertheless open the possibility of first measurements of cross sections in the range of several mb/sr, i.e., values obtained for elastic scattering at backward angles in the system $\alpha + {}^{40}$Ca.

The long half-life of ^{44}Ti ($T_{1/2} = 60$ yr) makes the production of either a ^{44}Ti beam or a ^{44}Ti target possible. However, because of the small amounts of ^{44}Ti material available, it is experimentally easier to use a ^{44}Ti beam and study elastic scattering in inverse kinematics by bombarding a ^{4}He target with a radioactive ^{44}Ti beam. After transforming the yields to the center-of-mass system the cross sections are independent of the chosen kinematics. Although a ^{4}He target was used in the experiment, the usual term "α scattering" will be used throughout the paper.

The ^{44}Ti material for the experiment was produced via the ^{45}Sc$(p, 2n)^{44}$Ti reaction [16,17] using a 50-MeV proton beam from the linac injector of the Argonne Intense Pulsed Neutron Source. A 25 mm diam, 5 mm thick disk of Sc, mounted in a water-cooled Cu holder behind a 7 mm thick graphite absorber, was bombarded for $\sim$3 days with a 20 μA proton beam. Two weeks after the irradiation the Sc disk was removed from the irradiation site and placed in front of a Ge detector. The ^{44}Ti activity corresponded to $\sim 1.3\ \mu$g of ^{44}Ti, equivalent to $\sim 1.8 \times 10^{16}$ atoms. Four weeks later the ^{44}Ti activity was chemically separated from the Sc material using the procedure described in Refs. [18,19]. A part of the active material, in the form of $^{44}TiO_2$, was then mixed with about 50 mg of $^{nat}TiO_2$ and pressed into the copper insert of a negative-ion Cs-sputter source. A beam of $^{44}TiO^-$ was extracted from the ion source and injected into the tandem accelerator at ATLAS. After stripping in the tandem, the 72 MeV $^{44}Ti^{8+}$ beam was accelerated to $E =$ 280 MeV in the superconducting linac part of ATLAS. To optimize the transmission through the accelerator, two guide beams were used. The ion source part of the accelerator was tuned using the stable $^{48}TiO^-$ molecule, while the linac was optimized with a $^{66}Zn^{12+}$ beam which has the same m/q value as $^{44}Ti^{8+}$. The average ^{44}Ti beam intensity measured on target was about 5×10^5 ^{44}Ti/s with roughly an equal amount of impurities from the stable isobar ^{44}Ca, which could not be separated by the beam transport system.

The ^{4}He target consisted of a 5 mm long gas cell with two 1.3 mg/cm^2 titanium windows, filled with 600 mbar of ^{4}He and cooled to liquid nitrogen temperature resulting in an areal density of about 60 μg/cm^2. The energy of the ^{44}Ti beam in the middle of the target was 261.5 MeV. The α particles were detected with an array of two 500 μm thick annular silicon strip detectors and a ΔE-E telescope at 0° (180° in the c.m. system). The annular detectors were segmented into 16 rings and 16 wedges allowing the determination of polar (θ) and azimuthal (ϕ) angles of the scattered particles. The detectors covered the angular range from 8° to 30° in the laboratory system ($\theta =$ 120°–164° in the center-of-mass system). Wedge-shaped polyethylene absorbers were mounted in front of the annular detectors to suppress the elastically scattered ^{44}Ti particles. Two Si detectors at $\theta_{\rm lab} = \pm 6°$ served to monitor the beam intensity and purity. For a separation of the ^{44}Ti and ^{44}Ca beam components the two detectors were covered with a 15.4 mg/cm^2 thick Au foil. The different energy loss rates in these foils resulted in an energy difference of 26.5 MeV and allowed for a clean separation of the two beam components in these monitor detectors.

The whole apparatus was tested with ^{28}Si and ^{40,44}Ca beams because angular distributions with α beams on ^{28}Si and ^{40,44}Ca targets had been measured previously [20,21]. The corrections of ^{44}Ca elastic scattering from the mixed ^{44}Ti/^{44}Ca beam measurements was obtained by performing a separate experiment with a pure ^{44}Ca beam under identical conditions, and subtracting the normalized yields from the spectra measured with the mixed beam.

The angular distributions of elastic scattering of α particles from ^{40}Ca ($E_{\rm lab} = 240$ MeV, $E_{\rm c.m.} = 21.8$ MeV) and ^{44}Ti ($E_{\rm lab} = 261.5$ MeV, $E_{\rm c.m.} = 21.8$ MeV) obtained in this experiment are compared in Fig. 1 (open and solid points, respectively). While for ^{40}Ca at angles close to 180° elastic cross sections higher than the Rutherford values were confirmed, the corresponding yields for ^{44}Ti are about a factor of 20 smaller and, thus, are comparable to the yields obtained for systems such as $\alpha +$ ^{42,44,48}Ca [21,22] or heavier nuclei. The solid lines are the result of an optical model fit that follows closely the analysis [8] which was successfully used in describing elastic alpha scattering on a few nuclei between ^{40}Ca and ^{208}Pb. The shape of the real part of the potential is calculated by the double-folding model of Ref. [23]:

$$V_f(r,E) = \lambda \iint dr_1 dr_2 \rho_1(r_1)\rho_2(r_2) \times t(E, \rho_1, \rho_2, s = r - r_1 + r_2), \qquad (1)$$

where r is the separation of the center-of-mass of the target and projectile, $\rho_{1,2}$ are the respective nucleon densities, and λ is the potential strength parameter which was left as a free variable. The density of ^{44}Ti was taken from Ref. [24]. For the nucleon-nucleon interaction $t(E,\rho,s)$ the density-dependent parametrization DDM3Y from Ref. [23] was chosen. With $\lambda = 1.28$ (see Table I) the central depth of this potential is $V(r=0) = -187.5$ MeV.

For the imaginary part a pure Woods-Saxon parametrization was chosen, and the parameters (potential depth $V_I = 16.9$ MeV, radius $R_I = 4.92$ fm, and diffuseness $a_I = 0.9$ fm) were adjusted to the new experimental data. In the case of ^{40}Ca the parameters are close to the values given in [8]. The 20% discrepancy of the rms

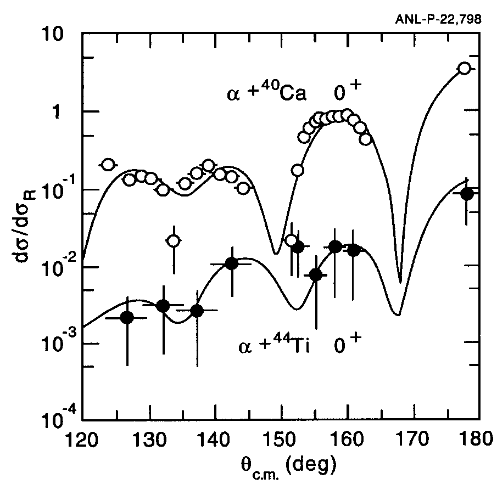

FIG. 1. Ratio between the differential cross sections for elastic scattering and the Rutherford values measured for the systems $\alpha +$ ^{40}Ca and $\alpha +$ ^{44}Ti at a center-of-mass energy of 21.8 MeV. The cross sections for the ^{44}Ti target are smaller than the ones for ^{40}Ca by 1–2 orders of magnitude. The solid lines are the result of optical model calculations using a double-folding potential for the real part and a Woods-Saxon parametrization for the imaginary part. See text for details.

TABLE I. Potential strength parameters (λ), volume integrals ($J_{R,I}$), and rms radii obtained from optical model fits to ^{4}He scattering data for various target nuclei (first column).

Nucleus	$E_{c.m.}$ (MeV)	λ	J_R (MeV fm^3)	$r_{rms,R}$ (fm)	J_I (MeV fm^3)	$r_{rms,I}$ (fm)	Reference
^{40}Ca	21.8	1.28	356	4.27	36.6	4.79	This work
^{40}Ca	26.5	1.33	363	4.27	33.4	3.99	Ref. [8]
^{44}Ti	21.8	1.28	357	4.39	64.0	5.06	This work
^{58}Ni	27.1	1.31	350	4.53	89.1	4.27	Ref. [8]

radius in the imaginary potential reflects typical uncertainties when the shape of the imaginary potential is extracted from scattering data at low energies (see, e.g., Figs. 5 and 6 of Ref. [25]). The smaller cross sections at backward angles for ^{44}Ti require a stronger absorptive potential, roughly twice as strong as for ^{40}Ca, but comparable to the results obtained for heavier nuclei such as ^{58,60}Ni [8]. Table I summarizes the strength parameters λ for the folding potential, the volume integrals, and the rms radii obtained from the least-squares fits. For comparison, results for other nuclei in this mass range are also included.

The large difference in the backward scattering of alpha particles on ^{40}Ca and ^{44}Ti can also be seen from a comparison of angle-integrated cross sections. In Fig. 2 angle-integrated cross sections for elastic scattering at backward angles are shown for several nuclei in the mass range $A = 32$–58 [26] measured at similar energies. The size of the squares is proportional to the yields

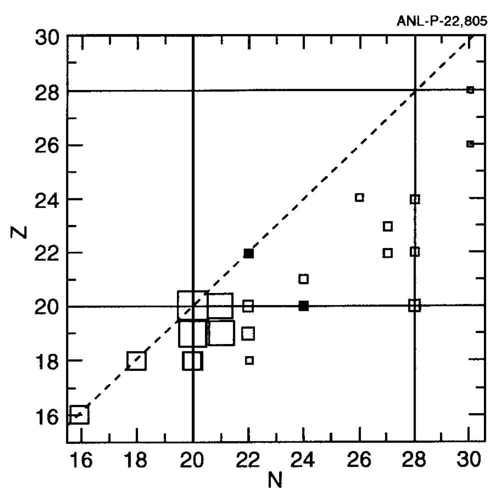

FIG. 2. Angle-integrated yields for elastic scattering of α particles at energies around 25 MeV on various targets between A=32 and 58 plotted in the (N, Z) plane. The size of the squares is proportional to the cross section integrated over the angular range $\theta_{c.m.} = 140°$–$180°$. The solid lines indicate the location of the magic neutron and proton numbers in this mass range. The dashed line follows the $Z = N$ nuclei. The solid squares are obtained from the present experiment, while the open squares are data taken from the literature.

integrated in the angular range $\theta_{c.m.} = 140°$–$180°$. The cross sections for ^{44}Ti and ^{44}Ca obtained in this experiment are given by the solid squares. Our result for ^{40}Ca is found to be in good agreement with the value taken from the literature [26]. As can be seen from Fig. 2, the largest backward yields are concentrated around the double magic nucleus ^{40}Ca with smaller cross sections observed for ^{42}Ca, ^{41}K, and ^{38,40}Ar. The new value for ^{44}Ti is considerably smaller than that for ^{40}Ca and comparable to other cross sections in this mass range (e.g., ^{44}Ca, ^{45}Sc). It also agrees with the general trend predicted by the optical model (see Ref. [26]).

The strong $B(E2)$ value of the first excited state in ^{44}Ti made it possible to also measure the angular distribution for inelastic excitation of the 2^+ state at $E_x = 1.083$ MeV, which is shown in Fig. 3 compared with the cross section of the elastic channel. The yields for inelastic scattering at backward angles are comparable to the elastic cross sections. Because no information is available for higher lying states from the present experiment, we have analyzed the data within the framework of the distorted-wave Born approximation (DWBA). The angular distribution from the DWBA calculation performed with the finite-range code PTOLEMY [27], using the optical potential

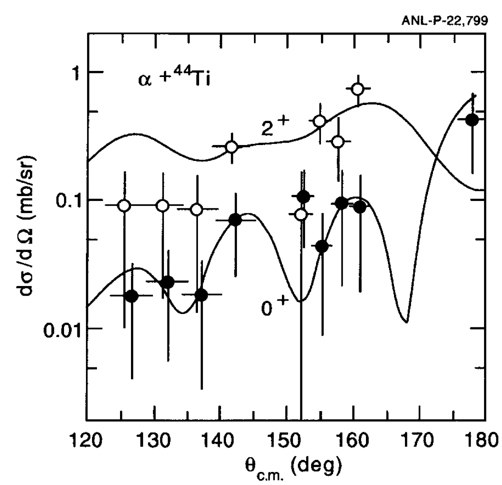

FIG. 3. Differential cross sections for elastic scattering (solid points) and inelastic excitation of the first 2^+ (open points) in ^{44}Ti. The solid lines are the result of optical model (elastic) and DWBA (inelastic) calculations described in the text.

from Fig. 2, a $B(E2) = 0.061e^2\ b^2$ [28]), and a nuclear deformation parameter $\beta = 0.2$ is shown by the solid line in Fig. 3. Similar to the results observed for the 2^+ excitation in the system $\alpha + {}^{44}$Ca, the ^{44}Ti data are in good agreement with the calculations. Attempts to reproduce the ^{44}Ti results in a coupled-channels analysis using the ^{40}Ca optical potential were not successful.

These first measurements of elastic and inelastic α scattering with an $N = Z$ nucleus heavier than ^{40}Ca have shown that the ALAS appears to stop at ^{40,41}Ca. An optical-model analysis of the $\alpha + {}^{44}$Ti data gave parameters which are in good agreement with the results obtained for scattering of α particles on heavier nuclei. The reduced absorption which is required to explain ALAS cannot originate from the (α, n) channel, since the Q values for the (α, n) reaction on ^{40}Ca and ^{44}Ti are both quite large and negative (-11.172 MeV and -8.642 MeV, respectively). As was already observed in Ref. [29], the backward enhancement is strongest for nuclei at the closure of major oscillator shells (e.g., ^{16}O and ^{40}Ca). This might be caused by the increase in the size of the wave functions at the beginning of a new oscillator shell. It would be interesting to investigate whether there is any enhancement in the backward angle scattering of alpha particles on ^{56}Ni, although no appreciable enhancement has been observed (see Fig. 2) for ^{48}Ca. However, the properties of ^{56}Ni beams at present accelerators, in particular, their intensity and the isobar contamination with ^{56}Co, are not suited for a measurement of elastic scattering, leaving this system for the next generation facilities.

We thank F. Brumwell, D.L. Bowers, and G. McMichael for their help in preparing the ^{44}Ti sample. This work was supported by the U.S. Department of Energy, Nuclear Physics Division, under Contract No. W-31-109-ENG-38.

[1] R. Planeta, H. Dabrowski, L. Freindl, and K. Grotowski, Nucl. Phys. **A326**, 97 (1979), and references cited therein.
[2] D. Agassi and N. S. Wall, Phys. Rev. C **7**, 1368 (1973).
[3] K.W. McVoy, Phys. Rev. C **3**, 1104 (1971).
[4] A. S. Rinat (Reiner), Phys. Lett. **38B**, 281 (1972).
[5] K. A. Eberhard, Phys. Lett. **33B**, 343 (1970).
[6] F. Michel and R. Vanderpoorten, Phys. Rev. C **16**, 142 (1977).
[7] H. P. Gubler, U. Kiebele, H. O. Meyer, G. R. Plattner, and I. Sick, Phys. Lett. **74B**, 202 (1978).
[8] U. Atzrott, P. Mohr, H. Abele, C. Hillenmayer, and G. Staudt, Phys. Rev. C **53**, 1336 (1996).
[9] F. Brau, F. Michel, and G. Reidemeister, Phys. Rev. C **57**, 1386 (1998).
[10] K. E. Rehm *et al.*, Nucl. Instrum. Methods Phys. Res., Sect. A **449**, 208 (2000).
[11] A. A. Sonzogni *et al.*, Phys. Rev. Lett. **84**, 1651 (2000).
[12] H. J. Apell *et al.*, Nucl. Phys. **A246**, 477 (1975).
[13] L.W. Put and A. M. J. Paans, Nucl. Phys. **291**, 93 (1977).
[14] P. Braun-Munzinger *et al.*, Phys. Rev. Lett. **38**, 944 (1977).
[15] M.C. Mermaz, M. A. G. Fernandes, A. Greiner, B.T. Kim, and N. Lisbona, Phys. Rev. C **19**, 794 (1979).
[16] T. McGee *et al.*, Nucl. Phys. **A150**, 11 (1970).
[17] R. Ejnisman *et al.*, Phys. Rev. C **54**, 2047 (1996).
[18] D. Frekers *et al.*, Phys. Rev. C **28**, 1756 (1983).
[19] R. Lange *et al.*, Nucl. Instrum. Methods Phys. Res., Sect. A **423**, 247 (1999).
[20] A.W. Obst and K.W. Kemper, Phys. Rev. C **6**, 1705 (1972).
[21] G. Gaul *et al.*, Nucl. Phys. **A137**, 177 (1969).
[22] W. Trombik, K. A. Eberhard, and J. S. Eck, Phys. Rev. C **11**, 685 (1975).
[23] A. M. Kobos, B. A. Brown, R. Lindsay, and R. Satchler, Nucl. Phys. **A425**, 205 (1984).
[24] R. Ejnisman *et al.*, Phys. Rev. C **58**, 2531 (1998).
[25] Zs. Fülöp *et al.*, Phys. Rev. C **64**, 065805 (2001).
[26] K.A. Eberhard, M. Wit, J. Schiele, W. Trombik, W. Zipper, and J.P. Schiffer, Phys. Rev. C **14**, 2332 (1976).
[27] D.H. Gloeckner, M.H. Macfarlane, and S.C. Pieper, Argonne National Laboratory Report No. ANL-76-11, 1978 (unpublished).
[28] S. Raman *et al.*, At. Data Nucl. Data Tables **36**, 1 (1987).
[29] H. Oeschler *et al.*, Phys. Rev. Lett. **28**, 694 (1972).